Molecular Bridging of Silicon Nanogaps

Geoffrey J. Ashwell,[†,‡,¶,*] Laurie J. Phillips,[‡,¶] Benjamin J. Robinson,[†,‡,¶] Barbara Urasinska-Wojcik,[‡,¶] Colin J. Lambert,[†] Iain M. Grace,[†] Martin R. Bryce,[§] Rukkiat Jitchati,[§,#] Mustafa Tavasli,[§,▲] Timothy I. Cox,[⊥] Ian C. Sage,[⊥] Rachel P. Tuffin,[⊥] and Shona Ray[∥]

[†]Physics Department, Lancaster University, Lancaster LA1 4YB, U.K., [‡]College of Physical and Applied Sciences, Bangor University, Gwynedd LL57 2UW, U.K., [§]Department of Chemistry, Durham University, Durham DH1 3LE, U.K., [⊥]QinetiQ plc, St. Andrews Road, Malvern WR14 3PS, U.K., and [∥]Semefab (Scotland) Ltd., Newark Road South, Glenrothes, Fife KY7 4NS, U.K. [¶]The Nanomaterials Group has transferred from Bangor to Lancaster University. [#]Current address: Department of Chemistry, Ubon Ratchathani University, Warinchumrap, Ubon Ratchathani 34190, Thailand. [▲]Current address: Department of Chemistry, Uludag University, 16059 Nilufer, Bursa, Turkey.

ARTICLE

ABSTRACT The highly doped electrodes of a vertical silicon nanogap device have been bridged by a 5.85 nm long molecular wire, which was synthesized *in situ* by grafting 4-ethynylbenzaldehyde *via* C—Si links to the top and bottom electrodes and thereafter by coupling an amino-terminated fluorene unit to the aldehyde groups of the activated electrode surfaces. The number of bridging molecules is constrained by relying on surface roughness to match the 5.85 nm length with an electrode gap that is nominally 1 nm wider and may be controlled by varying the reaction time: the device current increases from ≤1 pA at 1 V following the initial grafting step to 10—100 nA at 1 V when reacted for 5—15 min with the amino-terminated linker and 10 μA when reacted for 16—53 h. It is the first time that both ends of a molecular wire have been directly grafted to silicon electrodes, and these molecule-induced changes are reversible. The bridges detach when the device is rinsed with dilute acid solution, which breaks the imine links of the *in situ* formed wire and causes the current to revert to the subpicoampere leakage value of the 4-ethynylbenzaldehyde-grafted nanogap structure.

KEYWORDS: silicon nanogap · vertical nanogap electrode device · molecular electronics · molecular wire · self-assembled monolayer · stepwise synthesis

Noninvasive contacting is at the forefront of studies on molecular electronic materials,[1−7] but its exploitation depends upon the fabrication of nanometer-sized electrode gaps[8] and availability of self-assembling molecular wires whose lengths coincide with the widths to be bridged.[9−12] It represents the ultimate challenge in device miniaturization, but for commercial realization, if at all, it is necessary to develop scalable contacting technologies to provide a high density of molecular devices per single chip. We focus on sandwich structures in which the electrodes are separated by an insulating layer which is undercut to provide *vertical nanogap electrode devices*. There are few examples[12−20] with only one to date in which conjugated molecular wires are covalently bonded to the electrodes on opposite sides of the vertical gap. It comprises a Au/SiO_2/Si_3N_4/Au structure in which 3.5 nm long molecules connect top and bottom to the gold electrodes in a necklace arrangement around the perimeter of an insulating SiO_2/Si_3N_4 mushroom-shaped core.[12] Vertical nanogaps have also been bridged by molecule-connected nanoparticles[15] as well as by C_{60} and nanoparticulate deposits.[17,21]

Molecular electronics is still in its infancy, and considerable effort is required for the design and synthesis of appropriate materials and the development of scalable contacting techniques. Silicon is an emerging platform: the covalent grafting of molecules is well-established[22−25] and, although it is difficult to match the length of a molecule to the width of the electrode gap, molecular bridging may be achieved *in situ* by the stepwise coupling of chemical building blocks.[9−12] This highly versatile method combines ease of synthesis[26−33] with subnanometer control of molecular length and, in addition, provides a means of exploiting functionality by incorporating electroactive units (electron bridges, donors, and acceptors) at defined points along the molecular backbone of the stepwise-formed wire.[27,33]

In what follows, this modular approach is adapted to bridge silicon nanogaps and the devices provide evidence of long-term stability. Here we report the fabrication of vertical nanogap structures featuring two highly doped silicon microelectrodes with a nominal separation of 7 nm and molecular bridging by the *in situ* synthesis of conjugated wires within the nanogaps. To limit the number of bridges, we rely on surface roughness and molecular lengths that are *ca.* 1 nm shorter than the nominal width of the gap. This deliberate mismatch limits the number of working devices but provided the means to bridge the silicon electrodes *via* either a single molecule or few molecules. The molecule integrated Si—wire—Si structures exhibit a lower limiting current of *ca.* 10 nA at ±1 V.

*Address correspondence to g.j.ashwell@lancaster.ac.uk.

Received for review September 20, 2010 and accepted November 09, 2010.

Published online November 17, 2010. 10.1021/nn102460z

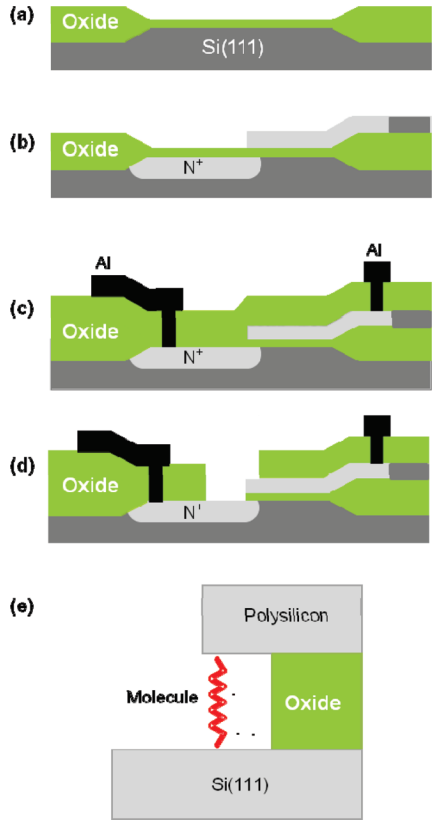

Figure 1. Microfabrication of a silicon nanogap structure: (a) growth of a 7 nm thick gate oxide layer on n-type Si(111) included in the LOCOS isolation process; (b) arsenic implantation to provide a highly doped N^+ channel in the substrate followed by deposition, patterning, and implantation of a polycrystalline silicon overlay on the preformed oxide; (c) deposition of low temperature oxide (LTO), patterning of contact holes, and deposition and etching of either platinum or aluminum plugs to act as contacts to each of the doped silicon electrodes; (d) patterning and etching of the LTO to expose the active area of the nanogap structure; (e) enlarged view of the active area after etching with NH_4F solution followed by molecular grafting and *in situ* reaction to provide a molecular bridge between the top and bottom electrodes. The height of the silicon nanogap is controlled by the thickness of the initially formed gate oxide layer.

RESULTS AND DISCUSSION

Complementary metal-oxide-semiconductor (CMOS) processing[14,15] is fundamental to our approach to mass produce electrode nanogaps[8] and, using process steps outlined in Figure 1, was employed here to fabricate vertical $Si/SiO_2/Si$ structures in which the lower and upper electrodes are highly doped Si(111) and polycrystalline Si, respectively, and the gate oxide layer is nominally 7 nm thick. The oxide layer was etched with NH_4F to expose and hydrogenate the silicon surfaces of an undercut nanogap (Figure 2) and reacted under argon with the diethylacetal derivative of 4-ethynylbenzaldehyde in hexadecane (0.1 mg cm^{-1}) for 2 h at 190 °C to protect the surface from oxidation. Devices were rinsed with chloroform to remove physisorbed material and with acidified solution to generate the aldehyde. Analytical studies confirm the covalent grafting of the 4-ethynylbenzaldehyde to Si(111)

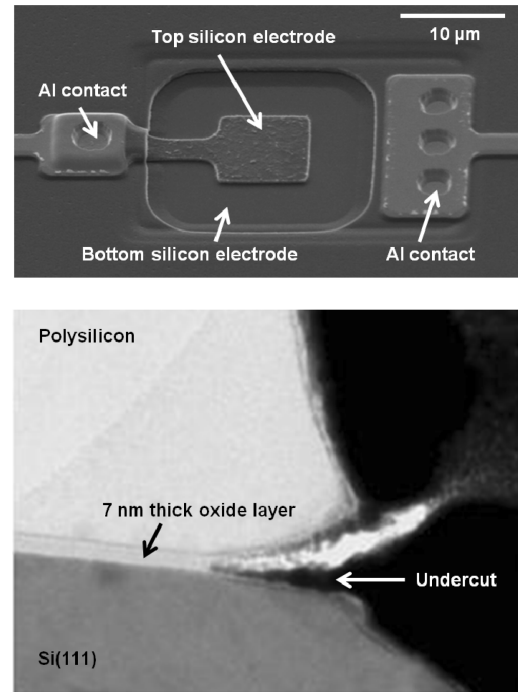

Figure 2. Magnified image of the silicon nanogap device structure (top) and TEM cross section of the electrode gap obtained by undercutting the gate oxide layer (bottom). Thickness variation along the length of the oxide layer is shown upon enlargement of the lower image, and this variation is significant at the molecular scale.

under these conditions. The silicon−organic interface, investigated by Fourier transform infrared attenuated total reflection spectroscopy (FTIR-ATR) of molecules grafted to planar silicon, exhibits stretching vibrations consistent with the grafted molecule (*e.g.*, ν_{CO} 1703 cm^{-1}) as well as a SiO_x contaminant[34] (Figure 3). Moreover, its X-ray photoelectron spectrum (XPS) exhibits a peak at 101.9 eV (Si 2p, Si−C) consistent with covalent grafting of the molecule[35] but whose maximum is influenced by a nearby shoulder at *ca.* 103 eV, which corresponds to the binding energy of the oxide contaminant.[36] Both the XPS and FTIR-ATR data conform to

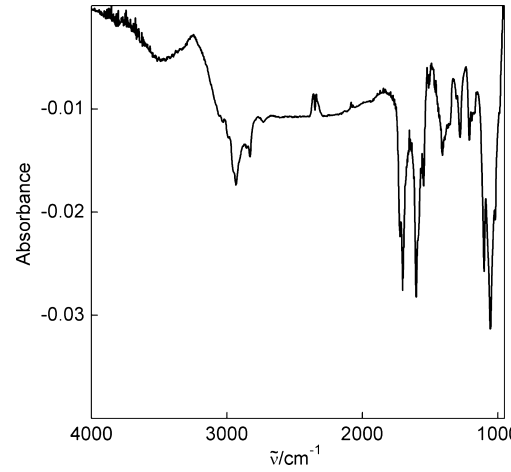

Figure 3. FTIR-ATR spectrum of 4-ethynylbenzaldehyde grafted to silicon: ν 1703 cm^{-1} (CO); 1604 cm^{-1} (C═C); 1057 cm^{-1} (SiO_x).

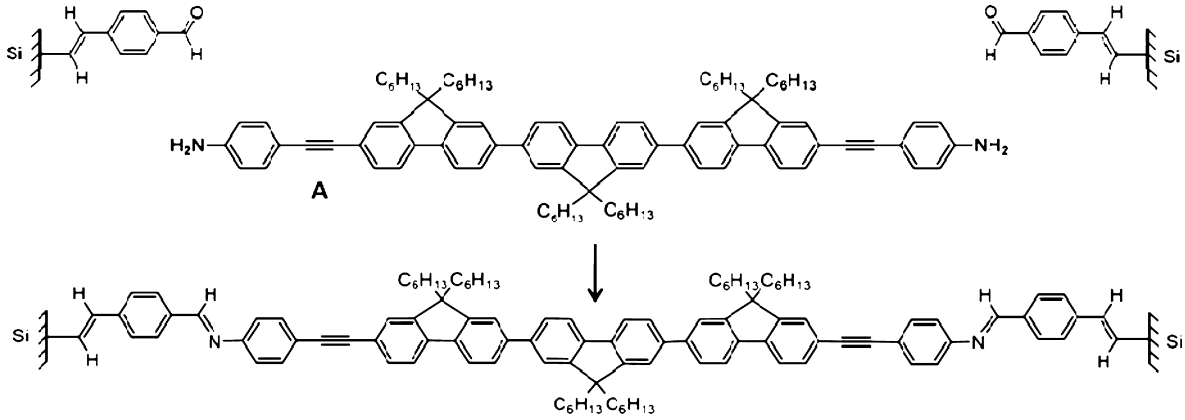

Figure 4. ***In situ*** **coupling with a 4 nm long amino-terminated linker (A) to bridge the silicon nanogap.**

moderately high coverage of the silicon substrate by the grafted molecule but also indicate partial oxidation of the surface. This is not problematic for the nanogap device which requires only a small overlapping region of electrode-grafted molecules to connect the top and bottom surface aldehyde groups to a diamino-substituted linker.

Si(111) was chosen because its external bond is normal to the surface and produces an upright orientation for the grafted coating [Si−CH═CH−C_6H_4−CHO)], which acts as a template for reacting amino-terminated units to bridge the nanogap. A 4 nm long fluorene linker (**A**) was chosen (Figure 4) and, albeit confirmed from studies on planar substrates, *in situ* coupling is manifested by a 1.3 eV shift of the N 1s binding energy when NH_2 (400.3 eV) converts to CH═N (399.0 eV).[37] To achieve bridging, the coated nanogap devices were immersed in chloroform solutions of the amino-terminated linker **A** (0.03 mg cm^{-3}) to which catalytic traces of glacial acetic acid were added. Different samples were exposed for 5 min to 53 h and rinsed with copious volumes of solvent to remove physisorbed material. Following this procedure, molecular bridging is apparent from changes in the electrical properties: empty devices and those with 4-ethynylbenzaldehyde covalently grafted to the silicon electrodes exhibit leakage currents of ≤1 pA at 1 V, whereas connection across the nanogap, by coupling linker **A** with the surface aldehyde groups on opposite sides, causes the current to increase by at least 4 orders of magnitude.

I−*V* characteristics of CMOS-based arrays of nanogap devices (675 devices on 23 chips) were investigated using a Keithley Instruments model 6430 subfemtoamp source meter with contact to the metallic pads of the individual structures made using a Wentworth manual probe station. Following grafting of 4-ethynylbenzaldehyde in hexadecane at 190 °C, 435 devices showed evidence of shorting and were excluded from further investigation. Another 50 shorted when immersed in chloroform solutions of linker **A**. Of the remainder, 166 showed no change in their electrical properties, which is consistent with the length of the molecular wire (5.85 nm) being incompatible with the nominal width of the silicon nanogap (*ca.* 7 nm). These dimensions should be matched, but we considered the discrepancy to be appropriate, as it was necessary to reduce the number of docking sites when attempting to bridge the electrodes by a single molecule. Only 24 nanogap structures showed currents indicative of molecular bridging, and for each of these, we relied upon surface roughness and an uneven oxide layer thickness to provide compatibility of the gap width for bridging. This approach reduced the quantity of bridged devices but afforded control of the number of connecting molecules. For example, devices immersed for 5−15 min yielded currents of *ca.* 10−100 nA at 1 V (Figure 5), where the lower threshold corresponds to a value approaching the single-molecule limit and the upper threshold to a few connecting molecular wires. In contrast, those reacted for 16−53 h yielded currents of *ca.* 10 μA at 1 V, characteristic of multiple molecular bridges. Our control studies provide evidence that the behavior is induced by the bridging molecules as it was found that these conductive devices revert to a current of *ca.*1 pA at 1 V when rinsed with dilute acid solution (acetic acid, 10^{-3} M), which displaces the amino-terminated fluorene linker. Moreover, silicon nanogap devices with 4-ethynylbenzaldehyde covalently grafted to the electrodes fail to exhibit current enhancement when reacted with amino-terminated molecules that are too short to bridge the coated silicon electrodes, or aniline (C_6H_4−NH_2), which is monosubstituted. Values of *ca.* 1 pA at 1 V were obtained in each case.

Of the 24 molecule-inserted silicon nanogap devices studied, two exhibited currents of *ca.* 10 nA at 1 V when reacted for 5 min with the amino-terminated linker, three gave currents of 20−100 nA when reacted from 5 to 15 min, and the remainder showed enhanced currents of *ca.* 10 μA, characteristic of multiple molecular bridges, for reaction periods of 16−53 h. The devices showed no significant variation in the magnitude of the current or the shape of the *I*−*V* curve when studied in air or under an inert atmosphere. Most exhibited reproducible characteristics without degradation when

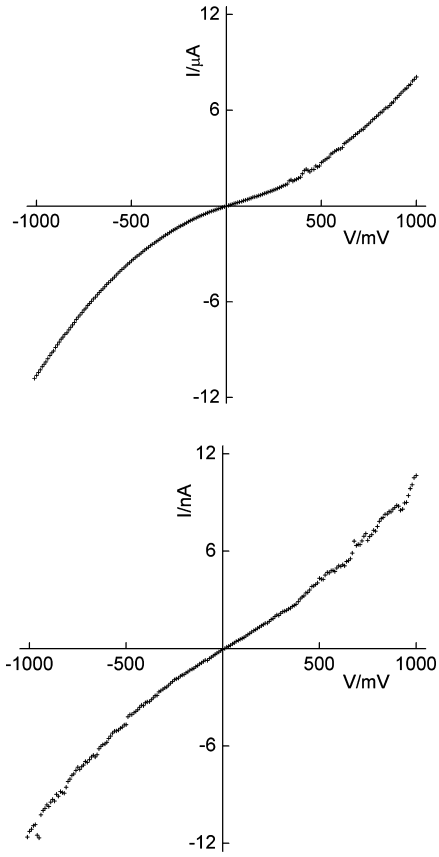

Figure 5. *I*−*V* characteristics of bridged silicon nanogap devices: (top) the current of *ca.* 10 μA at 1 V arises from multiple molecular bridges and was achieved following reaction for 53 h in a solution of the amino-terminated linker; (bottom) the current of *ca.* 10 nA at 1 V corresponds to the lower limit and was obtained following reaction for 5 min. For comparison, empty silicon devices and those grafted with 4-ethynylbenzaldehyde each display leakage currents of ≤1 pA at 1 V, and we note that the former, whose unprotected electrodes oxidize, shows no change in the electrical characteristics when immersed in solutions of amino-terminated linkers.

cycled between ±1 V, and from a limited study of a single device, there was no appreciable change when investigated six months after fabrication. All but one exhibited symmetrical or almost symmetrical *I*−*V* curves, and the slight electrical asymmetry of the nonconforming device may be attributed to a partial breakdown of the Si−(molecular wire)−Si structure during measurement. In each case, the *I*−*V* characteristics differ from those of shorted devices whose current is several orders of magnitude higher and varies linearly with voltage. Representative plots are included as Supporting Information.

The steep wedge-shaped undercut of the Si−SiO_2−Si nanogap (Figure 2) provides a narrow region of compatibility where the length of linker **A** coincides with the width of the gap reduced by the thickness of 4-ethynylbenzaldehyde grafted on each electrode. Surface roughness is fundamental to matching these dimensions, and although interdigitating arrangements cannot be excluded, limiting currents of *ca.*

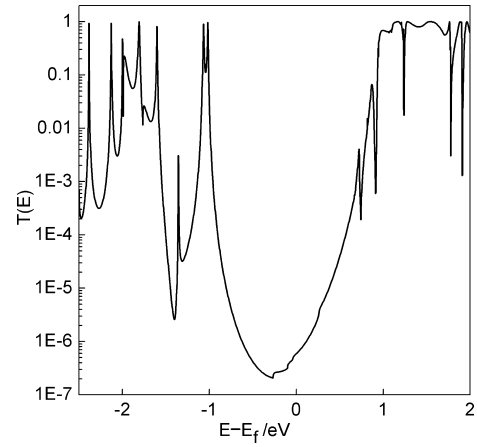

Figure 6. Theoretical transport properties of the molecule-inserted silicon nanogap: zero bias transmission coefficient of the molecular wire contacted by silicon leads as a function of $E - E_f$, where E_f is the Fermi energy and E is the energy of the transmitted electrons.

10 nA at 1 V have been obtained using wafers from different batches. This threshold value is therefore more likely to arise from a single molecular bridge rather than an interdigitating arrangement where there is no control of the size of the cluster. Moreover, the somewhat limited increase in current when the reaction time is increased from 5 min to 53 h (Figure 5) is consistent with the electrode area for bridging being restricted by the wedge-shaped undercut. The accessible area for interdigitation is greater: it is not limited by a precise gap width as there may be variable intermolecular overlap between molecules on opposite sides.

To predict the electrical transport properties of this molecular wire attached to silicon leads, we used the *ab initio* transport code SMEAGOL[38] and the density functional (DFT) code SIESTA.[39] First we calculated the relaxed geometry of the isolated molecule shown in Figure 4 using DFT and the optimum binding geometry of this molecule to the silicon surface. The molecule was then extended to include 6 layers of Si(111), each containing 25 atoms, which were attached to infinite periodic leads. Periodic boundary conditions were imposed in the *x* and *y* directions (the axis of transport is along the *z* axis).We chose a lead structure to mimic the doped behavior, that is, with a finite density of states at the Fermi energy. The zero bias electron transmission coefficient, $T(E)$, was then calculated using SMEAGOL and is shown in Figure 6. Here, the Fermi energy (0 eV) sits closer to the LUMO resonance, and the gap between the resonances is approximately 2 eV. The *I*−*V* relation, obtained from $T(E)$ using the following formula

$$I = \frac{2e}{h}\int_{-eV/2}^{eV/2} T(E)\mathrm{d}E$$

is shown in Figure 7. The theoretical curve shows a more pronounced reverse S-shape in contrast to the experimental *I*−*V* curves of Figure 5, which may be due

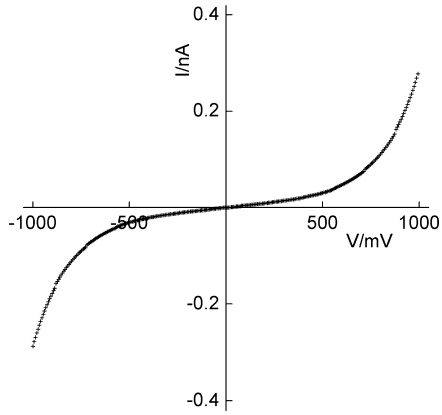

Figure 7. Theoretical *I*−*V* characteristics of the silicon-contacted molecular wire shown in Figure 4.

to higher voltage effects not included in the equilibrium calculation, and the conductance is lower than the experimentally determined limiting value. There may be more than a single bridging molecule. However, these discrepancies probably arise from well-known problems associated with the use of DFT to estimate the HOMO−LUMO gap and position of the Fermi energy as well as to difficulties in simulating molecule-integrated device characteristics when the electrodes of the nanogap structure are highly doped and asymmetric: the lower surface is Si(111), and the upper is polycrystalline Si. It leads to problems from a theoretical viewpoint as it makes it difficult to model a system with unknown parameters. Full details of the theoretical method can be found in the Supporting Information.

In conclusion, we have demonstrated the scalable fabrication of silicon nanogaps and achieved molecular bridging by the *in situ* stepwise synthesis of molecules within the gap. The limiting current of 10 nA at 1 V (*cf.* 0.3 nA from theory for a single molecule) may be assigned to a small number of molecular bridges, although a single molecule contact cannot be ruled out as the simulated value was obtained using silicon leads instead of the arsenic-doped silicon contacts used in the experimental study. It is the first time that both ends of a molecule have been grafted to silicon, but there have been previous reports of the electrical characterization of silicon nanogaps bridged by alkanethiolate-connected gold nanoparticles[15] and C_{60} deposits[21] as well as monolayer-coated silicon nanowires in physical contact with silicon pads.[40] These few examples differ from the undercut Si−SiO_2−Si device structure shown here in which a conjugated molecular wire bridges the nanometer-sized gap and covalently bonds to the highly doped silicon electrodes *via* Si−C linkages on opposite sides.

Acknowledgment. We thank the Technology Strategy Board, EC FP7 ITN "FUNMOLS" Project No. 212942 and EPSRC for financial support and Jean-Noel Chazalviel (Ecole Polytechnique, Paris) for FTIR studies on 4-ethynylbenzaldehyde grafted to Si.

Supporting Information Available: Synthetic methods; analytical data; *I*−*V* characteristics of an empty silicon nanogap device, a shorted device, and various bridged devices; theoretical calculations. This material is available free of charge *via* the Internet at http://pubs.acs.org.

REFERENCES AND NOTES

1. Li, T.; Hu, W.; Zhu, D. Nanogap Electrodes. *Adv. Mater.* **2010**, *22*, 286–300.
2. Moth-Poulsen, K.; Bjørnholm, T. Molecular Electronics with Single Molecules in Solid-State Devices. *Nat. Nanotechnol.* **2009**, *4*, 551–556.
3. Wu, S.; González, M. T.; Huber, R.; Grunder, S.; Mayor, M.; Schönenberger, C.; Calame, M. Molecular Junctions Based on Aromatic Coupling. *Nat. Nanotechnol.* **2008**, *3*, 569–574.
4. Tsutsui, K.; Nakata, M.; Morita, M.; Tokuda, M.; Nagatsuma, K.; Onozato, H.; Kaneko, T.; Edura, T.; Mita, Y.; Koinuma, H.; *et al.* Novel Fabrication Technologies of Planar Nano-Gap Electrodes for Single Molecule Evaluation. *Curr. Appl. Phys.* **2007**, *7*, 329–333.
5. Tao, N. J. Electron Transport in Molecular Junctions. *Nat. Nanotechnol.* **2006**, *1*, 173–181.
6. Haiss, W.; Wang, C.; Grace, I.; Batsanov, A. S.; Schiffrin, D. J.; Higgins, S. J.; Bryce, M. R.; Lambert, C. J.; Nichols, R. J. Precision Control of Single-Molecule Electrical Junctions. *Nat. Mater.* **2006**, *5*, 995–1002.
7. Scott, A.; Janes, D. B.; Risko, C.; Ratner, M. A. *In Situ* Structural Characterization of Metal−Molecule−Silicon Junctions Using Backside Infrared Spectroscopy. *Appl. Phys. Lett.* **2007**, *91*, 033508.
8. Ashley, T.; Bruson, K. M.; Buckle, P. D.; Cox, T. I.; Geddes, N. J.; Jefferson, J. H.; Noble, R. A.; Sage, I. C.; Combes, D. J. A Molecular Single Electron Transistor (MSET) Detector Device. Int. Pat. Appl. PCT/GB2004/004699; Pub. No. 2005, WO 2005/048350, 2004.
9. Taniguchi, M.; Nojima, Y.; Yokota, K.; Terao, J.; Sato, K.; Kambe, N.; Kawai, T. Self-Organized Interconnect Method for Molecular Devices. *J. Am. Chem. Soc.* **2006**, *128*, 15062–15063.
10. Tang, J.; Wang, Y.; Klare, J. E.; Tulevski, G. S.; Wind, S. J.; Nuckolls, C. Encoding Molecular-Wire Formation within Nanoscale Sockets. *Angew. Chem., Int. Ed.* **2007**, *46*, 3892–3895.
11. Chen, X.; Braunschweig, A. B.; Wiester, M. J.; Yeganeh, S.; Ratner, M. A.; Mirkin, C. A. Spectroscopic Tracking of Molecular Transport Junctions Generated by Using Click Chemistry. *Angew. Chem., Int. Ed.* **2009**, *48*, 5178–5181.
12. Ashwell, G. J.; Wierzchowiec, P.; Bartlett, C. J.; Buckle, P. D. Molecular Electronics: Connection Across Nano-Sized Electrode Gaps. *Chem. Commun.* **2007**, 1254–1256.
13. Krahne, R.; Yacoby, A.; Shtrikman, H.; Bar-Joseph, I.; Dadosh, T.; Sperling, J. Fabrication of Nanoscale Gaps in Integrated Circuits. *Appl. Phys. Lett.* **2002**, *81*, 730–732.
14. Berg, J.; Che, F.; Lundgren, P.; Enoksson, P.; Bengtsson, S. Electrical Properties of Si−SiO_2−Si Nanogaps. *Nanotechnology* **2005**, *16*, 2197–2202.
15. Howell, S. W.; Dirk, S. M.; Childs, K.; Pang, H.; Blain, M.; Simonson, R. J.; Tour, J. M.; Wheeler, D. R. Mass-Fabricated One-Dimensional Silicon Nanogaps for Hybrid Organic/Nanoparticle Arrays. *Nanotechnology* **2005**, *16*, 754–758.
16. Dirk, S. M.; Howell, S. W.; Zmuda, S.; Childs, K.; Blain, M.; Simonson, R. J.; Wheeler, D. R. Novel One-Dimensional Nanogap Created with Standard Optical Lithography and Evaporation Procedures. *Nanotechnology* **2005**, *16*, 1983–1985.
17. Strobel, S.; Hernández, R. M.; Hansen, A. G.; Tornow, M. Silicon Based Nanogap Device for Studying Electrical Transport Phenomena in Molecule−Nanoparticle Hybrids. *J. Phys.: Condens. Matter* **2008**, *20*, 374126.
18. Strobel, S.; Arinaga, K.; Hansen, A.; Tornow, M. A Silicon-on-Insulator Vertical Nanogap Device for Electrical Transport Measurements in Aqueous Electrolyte Solution. *Nanotechnology* **2007**, *18*, 295201.

19. Luber, S. M.; Zhang, F.; Lingitz, S.; Hansen, A. G.; Scheliga, F.; Thorn-Csanyi, E.; Bichler, M.; Tornow, M. High-Aspect-Ratio Nanogap Electrodes for Averaging Molecular Conductance Measurements. *Small* **2007**, *3*, 285–289.
20. Im, H.; Huang, X.-J.; Gu, B.; Choi, Y. K. A Dielectric-Modulated Field-Effect Transistor for Biosensing. *Nat. Nanotechnol.* **2007**, *2*, 430–434.
21. Corley, D. A.; He, T.; Tour, J. M. Two-Terminal Molecular Memories from Solution-Deposited C_{60} Films in Vertical Silicon Nanogaps. *ACS Nano* **2010**, *4*, 1879–1888.
22. Aswal, D. K.; Koiry, S. P.; Jousselme, B.; Gupta, S. K.; Palacin, S.; Yakhmi, J. V. Hybrid Molecule-on-Silicon Nanoelectronics: Electrochemical Processes for Grafting and Printing of Monolayers. *Physica E* **2009**, *41*, 325–344.
23. Stewart, M. P.; Maya, F.; Kosynkin, D. V.; Dirk, S. M.; Stapleton, J. J.; McGuiness, C. L.; Allara, D. L.; Tour, J. M. Direct Covalent Grafting of Conjugated Molecules onto Si, GaAs and Pd Surfaces from Aryldiazonium Salts. *J. Am. Chem. Soc.* **2003**, *126*, 370–378.
24. Duclairoir, F.; Dubois, L.; Calborean, A.; Fateeva, A.; Fleury, B.; Kalaiselvan, A.; Marchon, J.-C.; Maldivi, P.; Billon, M.; Bidan, G.; *et al.* Bistable Molecules Development and Si Surface Grafting: Two Chemical Tools Used for the Fabrication of Hybrid Molecule/Si CMOS Component. *Int. J. Nanotechnol.* **2010**, *7*, 719–737.
25. He, T.; Corley, D. A.; Lu, M.; Di Spigna, N. H.; He, J.; Nackashi, D. P.; Franzon, P. D.; Tour, J. M. Controllable Molecular Modulation of Conductivity in Silicon-Based Devices. *J. Am. Chem. Soc.* **2009**, *131*, 10023–10030.
26. Rosink, J. J. W. M.; Blauw, M. A.; Geerligs, L. J.; van der Drift, E.; Rousseeuw, B. A. C.; Radelaar, S. Self-Assembly of π-Conjugated Azomethine Oligomers by Sequential Deposition of Monomers from Solution. *Langmuir* **2000**, *16*, 4547–4553.
27. Ashwell, G. J.; Wierzchowiec, P.; Phillips, L. J.; Collins, C.; Gigon, J.; Robinson, B. J.; Finch, C. M.; Grace, I. M.; Lambert, C. J.; Buckle, P. D.; *et al.* Functional Molecular Wires. *Phys. Chem. Chem. Phys.* **2008**, *10*, 1859–1866.
28. Luo, Y.; Piantek, M.; Miguel, J.; Bernien, M.; Kuch, W.; Haag, R. *In-Situ* Formation and Detailed Analysis of Imine Bonds for the Construction of Conjugated Aromatic Monolayers on Au(111). *Appl. Phys. A: Mater. Sci. Process.* **2008**, *93*, 293–301.
29. Choi, S. H.; Kim, B. S.; Frisbie, C. D. Electrical Resistance of Long Conjugated Molecular Wires. *Science* **2008**, *320*, 1482–1486.
30. Choi, S. H.; Risko, C.; Ruiz Delgado, M. C.; Kim, B.; Bredas, J.-L.; Frisbie, C. D. Transition from Tunneling to Hopping Transport in Long, Conjugated Oligo-imine Wires Connected to Metals. *J. Am. Chem. Soc.* **2010**, *132*, 4358–4368.
31. Luo, L.; Frisbie, C. D. Length-Dependent Conductance of Conjugated Molecular Wires Synthesized by Stepwise "Click" Chemistry. *J. Am. Chem. Soc.* **2010**, *132*, 8854–8855.
32. Tuccitto, N.; Ferri, V.; Cavazzini, M.; Quici, S.; Zhavnerko, G.; Licciardello, A.; Rampi, M. A. Highly Conductive ~40-nm-long Molecular Wires Assembled by Stepwise Incorporation of Metal Centres. *Nat. Mater.* **2009**, *8*, 41–46.
33. Ashwell, G. J.; Urasinska-Wojcik, B.; Phillips, L. J. *In Situ* Stepwise Synthesis of Functional Multijunction Molecular Wires on Gold Electrodes and Gold Nanoparticles. *Angew. Chem., Int. Ed.* **2010**, *49*, 3508–3512.
34. Amekura, H.; Umeda, N.; Kishimoto, N. Near-Surface Sensitive Infrared Reflection Spectroscopy on SiO_2 Implanted with High-Flux Negative Ions. *Vacuum* **2004**, *74*, 549–553.
35. Dufour, G.; Rochet, F.; Stedile, F. C.; Poncey, C.; de Crescenzi, M.; Gunnella, R.; Froment, M. SiC Formation by Reaction of Si(001) with Acetylene: Electronic Structure and Growth Mode. *Phys. Rev. B* **1997**, *56*, 4266–4287.
36. Hofman, R.; Westheim, J. G. F.; Pouwel, I.; Fransen, T.; Gellings, P. J. FTIR and XPS Studies on Corrosion-Resistant SiO_2 Coatings as a Function of the Humidity During Deposition. *Surf. Interface Anal.* **1996**, *24*, 1–6.
37. The binding energies are consistent with values reported in the National Institute of Standards and Technology (NIST) XPS database (http://srdata.nist.gov/xps/default.aspx).
38. Rocha, A. R.; Garcia-Suarez, V. M.; Bailey, S.; Lambert, C.; Sanvito, S.; Ferrer, J. Spin and Molecular Electronics in Atomically Generated Orbital Landscapes. *Phys. Rev. B* **2006**, *73*, 085414.
39. Soler, J. M.; Artacho, E.; Gale, J. D.; Garcia, A.; Junquera, J.; Ordejon, P.; Sanchez-Portal, D. The SIESTA Method for *Ab Initio* Order-N Materials Simulation. *J. Phys.: Condens. Matter* **2002**, *14*, 2745–2779.
40. Haight, R.; Sekaric, L.; Afzali, A.; Newns, D. Controlling the Electronic Properties of Silicon Nanowires with Functional Molecular Groups. *Nano Lett.* **2009**, *9*, 3165–3170.